Journal of Cerebral Blood Flow & Metabolism (2010) 30, 827–836

www.jcbfm.com

# Hypertension-induced vascular remodeling contributes to reduced cerebral perfusion and the development of spontaneous stroke in aged SHRSP rats

Erica C Henning[1,2], Steven Warach[1,2] and Maria Spatz[2,3]

[1]*Section on Stroke Diagnostics and Therapeutics, National Institute of Neurological Disorders and Stroke, National Institutes of Health, Bethesda, Maryland, USA;* [2]*Stroke Branch, National Institute of Neurological Disorders and Stroke, National Institutes of Health, Bethesda, Maryland, USA;* [3]*Trauma & Resuscitative Medicine, Naval Medical Research Center, Silver Spring, Maryland, USA*

**Stroke in spontaneously-hypertensive, stroke-prone (SHRSP) rats is of particular interest because the pathogenesis is believed to be similar to that in the clinical setting. In this study, we employed multi-modal MRI—ASL, DWI, $T_2$, GRE, $T_1$ (pre/post contrast)—to investigate the natural history of spontaneous cerebral infarction and the specific role of cerebral perfusion in disease development. Twelve female SHRSP rats (age: ~1 year) were imaged within 1 to 3 days of symptom onset. The distribution of ischemic lesions was the following: 28.1% visual, 21.9% striatal, 18.8% motorsensory, 12.5% thalamic, 12.5% auditory, 3.1% frontal/prelimbic, and 3.1% multiple areas. Ischemic lesions had significantly reduced blood flow in comparison with healthy tissue. Ischemic lesions were characterized by hyperplastic, thrombosed, and compressed vessels. These findings suggest that ischemic lesion development is related to hypertension-induced vascular remodeling and persistent hypoperfusion. This model should be useful for studying the relationship between chronic hypertension and subsequent stroke, both in terms of primary and secondary prevention.**
*Journal of Cerebral Blood Flow & Metabolism* (2010) **30,** 827–836; doi:10.1038/jcbfm.2009.246; published online 2 December 2009

**Keywords:** ASL; hypertension; MRI; perfusion; SHRSP; stroke

## Introduction

Spontaneously-hypertensive, stroke-prone (SHRSP) rats are of particular interest because their pathophysiology is similar to that of acute stroke patients presenting in the clinic. First developed in 1974 by Okamoto *et al* (Okamoto *et al*, 1974), SHRSP rats are a genetic model of severe hypertension with alterations in the renin–angiotensin (Hilbert *et al*, 1991; Kim *et al*, 1992) and endothelin systems (Jesmin *et al*, 2007; Savage and Jeng, 2002). These alterations contribute to the spontaneous development of cerebrovascular pathology in >80% of animals, on average, around 9 months of age (Yamori *et al*, 1976*a*; Yamori and Horie, 1977). Disease etiology includes cerebral lesions (ischemic or vasogenic in origin), hemorrhage, and white matter rarefaction. The brain is not the only organ affected; this particular strain also develops associated kidney, heart, and lung disease (Masineni *et al*, 2005).

Despite the plethora of studies investigating the natural history of stroke in SHRSP rats, the precise mechanism(s) of disease development remain poorly understood. Early studies concentrated on the histopathological characterization of cerebral lesions in aged animals on a normal diet, reporting presence of atherosclerotic plaque, medial degeneration, fibrinoid necrosis, hypertrophy, and thrombosis (Yamori *et al*, 1976*a*). However, when fed a high-salt diet, disease development may be accelerated by raising peripheral resistance and increasing blood pressure (BP). This change in diet takes advantage of the

Correspondence: Dr EC Henning, Section on Stroke Diagnostics and Therapeutics, Stroke Branch, National Institute of Neurological Disorders and Stroke, National Institutes of Health, Building 10, Room B1D733, 10 Center Drive, MSC 1063, Bethesda, MD 20892, USA.
E-mail: henninge@ninds.nih.gov
Portions of this work were presented at the International Cerebral Vascular Biology Conference, Ottawa, Ontario, Canada, July 2007, and the International Stroke Conference, San Diego, California, February 2009.
Received 26 August 2009; revised 31 October 2009; accepted 3 November 2009; published online 2 December 2009

# Report Documentation Page

*Form Approved*
*OMB No. 0704-0188*



| 1. REPORT DATE | 2. REPORT TYPE | 3. DATES COVERED |
|---|---|---|
| **OCT 2009** | | **00-00-2009 to 00-00-2009** |

| 4. TITLE AND SUBTITLE | 5a. CONTRACT NUMBER |
|---|---|
| **Hypertension-induced vascular remodeling contributes to reduced cerebral perfusion and the development of spontaneous stroke in aged SHRSP rats** | 5b. GRANT NUMBER |
| | 5c. PROGRAM ELEMENT NUMBER |
| 6. AUTHOR(S) | 5d. PROJECT NUMBER |
| | 5e. TASK NUMBER |
| | 5f. WORK UNIT NUMBER |
| 7. PERFORMING ORGANIZATION NAME(S) AND ADDRESS(ES) **Naval Medical Research Center,Trauma & Resuscitative Medicine,503 Robert Grant Avenue,Silver Spring,MD,20910** | 8. PERFORMING ORGANIZATION REPORT NUMBER |
| 9. SPONSORING/MONITORING AGENCY NAME(S) AND ADDRESS(ES) | 10. SPONSOR/MONITOR'S ACRONYM(S) |
| | 11. SPONSOR/MONITOR'S REPORT NUMBER(S) |

12. DISTRIBUTION/AVAILABILITY STATEMENT
**Approved for public release; distribution unlimited**

13. SUPPLEMENTARY NOTES

14. ABSTRACT

15. SUBJECT TERMS

| 16. SECURITY CLASSIFICATION OF: | | | 17. LIMITATION OF ABSTRACT | 18. NUMBER OF PAGES | 19a. NAME OF RESPONSIBLE PERSON |
|---|---|---|---|---|---|
| a. REPORT | b. ABSTRACT | c. THIS PAGE | | | |
| **unclassified** | **unclassified** | **unclassified** | **Same as Report (SAR)** | **10** | |

increased salt-sensitivity of the SHR and SHRSP strains, a direct result of alterations in $Na^+/H^+$ exchange (Orlov *et al*, 2000) and $Na^+/K^+/2Cl^-$ co-transport (Sonalker *et al*, 2004). Many have employed this method, feeding 4- to 6-week-old SHRSP rats 1.0% NaCl in drinking water, resulting in disease development 1 to 2 months later (Blezer *et al*, 1998*b*; Guerrini *et al*, 2002; Sironi *et al*, 2001). This means that cerebral lesions are occurring as early as 3 months of age. With this method, the question arises as to whether disease development is merely accelerated, or whether the spontaneous development of stroke on a normal diet occurs via a completely separate mechanism as when fed a high-salt diet.

To date, two major mechanisms of disease development have been suggested (Figure 1). The first (left path) may be coined progressive, in which the presence of chronic hypertension induces vascular remodeling and reduced cerebral blood flow (CBF) (Mies *et al*, 1999; Yamori *et al*, 1976*b*; Yamori and Horie, 1977). Hypertrophy (medial thickening) and eutrophy (luminal narrowing) lead to increased vascular resistance and wall sheer rates. As the vessels become less functionally responsive and more extensively filled with atherosclerotic plaque, there is risk for vascular compression and thrombi. In this case, ischemic lesion development occurs, followed by subacute development of cerebral edema and blood–brain barrier (BBB) disruption. In contrast, the second (right path) occurs more quickly and is akin to hypertensive encephalopathy (Fredriksson *et al*, 1985; Smeda *et al*, 1999; Tamaki *et al*, 1984). With an acute spike in BP, there is loss of CBF autoregulation and increased CBF. In this case, BBB disruption occurs, followed by extravasation of serum proteins and significant vasogenic edema (Blezer *et al*, 1998*b*; Sironi *et al*, 2001, 2004).

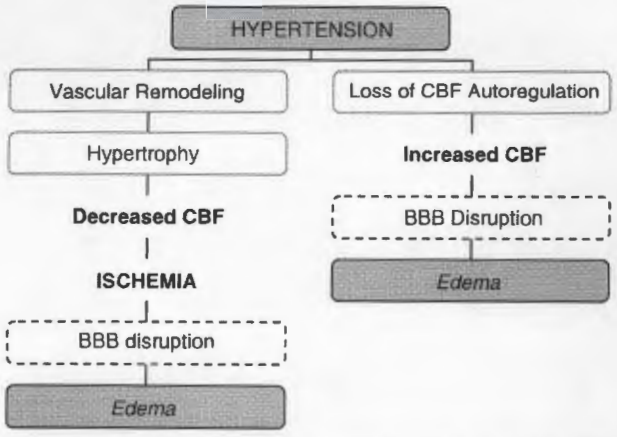


**Figure 1** Mechanisms of lesion development in SHRSP rats. 'Slow' development of disease occurs via vascular remodeling, hypertrophy, and hypoperfusion. In this setting, lesions develop first, followed by BBB disruption and formation of edema. 'Fast' development of disease occurs via an acute spike in BP, resulting in hyperperfusion. In this setting, BBB disruption and edema occur first, followed by vascular compression and hypoperfusion.

In this study, we employed multimodal magnetic resonance imaging (MRI) with continuous arterial spin labeling (ASL) to investigate the natural history of spontaneous cerebral infarction and the specific role of cerebral perfusion in disease development in aged SHRSP rats. Histology and immunohistochemistry were performed to validate MRI findings. We hypothesize that disease development is largely ischemic, related to hypertension-induced vascular remodeling and impaired cerebral perfusion.

## Materials and methods

### Animal Preparation and Monitoring

This study was approved by the institutional animal care and use committee (IACUC) of the National Institute of Neurological Disorders and Stroke, National Institutes of Health (IACUC protocol no. 1225-05). At approximately 6 months of age, 12 female SHRSP rats (bred from rats donated by Masahisa Kyogoku, MD, PhD, Kyoto-University, Kyoto, Japan) were monitored on a daily basis for alterations in neurological status (decreased spontaneous activity, mild incoordination, falling to one side, hunched posture, ruffled fur), signs of inflammation (porphyrin staining on one or both eyes), and decreased body weight (>5% body weight loss). The animals were provided free access to standard rat chow and water. Additional jello treat supplements were provided on a daily basis on the cage floor.

After development of stroke symptoms, animals were anesthetized with isoflurane (5% induction, 2.5% maintenance) delivered in a 2:2:1 mixture of breathing-quality air, nitrogen, and oxygen. The animal's head was secured using a stereotactic frame equipped with ear and bite bars. Body temperature was maintained at 37.0°C ± 0.5°C using an electrically heated bed (Rapid Biomedical GmbH, Rimpar, Germany). Heart rate and arterial oxygen saturation ($spO_2$) were continuously measured with a pulse oximeter (Surgivet, Waukesha, WI, USA) placed on the right hind paw.

### Magnetic Resonance Imaging

Imaging was performed using a Bruker Biospin 7.0 T/30 cm MRI system (Bruker Biospin, Billerica, MA, USA). A three-coil setup was employed for imaging. An in-house, transmit-only, birdcage, volume RF coil and a commercial, quadrature receive-only, surface RF coil (Rapid Biomedical GmbH, Rimpar, Germany) were used for all imaging. An additional in-house figure-8 labeling coil placed on the animal's neck was used for RF labeling of the blood in both common carotid arteries. Diffusion-weighted echo-planar imaging and $T_2$-weighted imaging were performed for assessment of cytotoxic and vasogenic edema. Continuous ASL was performed for assessment of cerebral perfusion. Gradient-echo imaging (GRE) was performed for identification of hemorrhage. $T_1$-weighted imaging ($T_1$WI) was performed pre/post contrast agent administration (0.2 mL gadolinium (Gd–DTPA at 0.5 mmol/L, intravenous;

Magnevist, Berlex Laboratories, Wayne, NJ, USA) for assessment of BBB integrity.

All images were acquired using a field of view = 2.56 cm × 2.56 cm. For diffusion-weighted echo-planar imaging: matrix size = 96 × 96; slice thickness = 1.5 mm, number of slices = 12; TR/TE = 6200/46 ms; $\Delta$ = 13 ms; $\delta$ = 4 ms; *b*-values = 0, 250, 500, 750, 1000 s/mm$^2$ (acquired for all three principle directions, *x*, *y*, *z*); four averages. For ASL: matrix size = 96 × 96; slice thickness = 1.5 mm; number of slices = 10; TR/TE = 5115/38 ms; label = 4183 ms; post-label = 350 ms; 32 averages. For $T_2$-weighted imaging: matrix size = 128 × 128; slice thickness = 1.5 mm, number of slices = 12; TR = 2000 ms; 8 echoes (15 ms → 120 ms); 1 average. For GRE: matrix size = 256 × 256; slice thickness = 1.0 mm, number of slices = 18; TR/TE = 350/12 ms; flip angle = 30°; 2 averages. For $T_1$WI: matrix size = 256 × 256; slice thickness = 1.5 mm; number of slices = 12; TR/TE = 245/4 ms; flip angle = 30°; 2 averages.

## Histopathology and Immunohistochemistry

After final imaging, 1.0 cc of 2.0% (w/v) Evan's Blue (EB) (E2129; Sigma, St Louis, MO, USA) was administered intravenously and allowed to circulate for 1 to 2 h. After an overdose of anesthesia (5% isoflurane), the animals were transcardially perfused with 0.9% (w/v) physiologically buffered saline for 5 min and 4.0% (w/v) paraformaldehyde for 15 min. Brains were extracted and placed in 4% paraformaldehyde for 1 to 2 days and then transferred to 20% sucrose overnight. They were then snap frozen in isopentane and stored at −73°C. Serial 16-$\mu$m-thick sections were taken beginning at the olfactory bulb and extending to the start of the cerebellum. For every set of 10 slides, the cryostat was advanced 500 $\mu$m. Hematoxylin–eosin staining was performed for identification of lesions and hemorrhages. Adjacent sections were evaluated for EB extravasation and fluorescence. Additional immunohistochemical experiments were performed to assess the status of the vascular/microvascular endothelium (Reca-1) and the extracellular matrix (laminin). Primary antibodies were obtained from Abcam (Cambridge, MA, USA). Secondary antibodies were obtained from Invitrogen (Carlsbad, CA, USA). Briefly, double immunofluorescence was performed for laminin (1:200, ab11575) and Reca-1 (1:100, ab22492) using AlexaFluor 488 (1:200, green) and AlexaFluor 546 (1:100, red) conjugated secondary antibodies.

## Image Analysis: MRI

Image analysis and parameter map production were performed using routines written in IDL (Research Systems Inc., Boulder, CO, USA). Apparent diffusion coefficient (ADC) and $T_2$ parameter maps were produced based on the relationship between the natural log of the signal intensity and *b*-value (equation (1)) or signal intensity and TE (equation (2)):

$$M(t) = M_0 e^{-b \cdot ADC_{avg}} \quad (1)$$

$$M(t) = M_0 e^{-TE/T_2} \quad (2)$$

where $M(t)/M_0$ is the signal intensity at a particular *b*-value or TE value, $ADC_{avg}$ is the average ADC across the three principle directions (*x*, *y*, *z*), and $T_2$ is the spin–spin relaxation time. A linear fitting procedure based on minimization of the $\chi^2$-statistic was performed for extraction of MR parameters. Quantitative CBF maps were generated using the following equation (Silva and Kim, 1999):

$$CBF = \frac{\lambda}{T_1} \frac{M_b^0 - M_b^{SS}}{M_b^{SS} + (2\alpha - 1)M_b^0} \quad (4)$$

where $\lambda$ is the brain/blood partition coefficient (0.9 mL/g); $T_1$ is the longitudinal relaxation time of the brain water magnetization in the absence of perfusion and cross-relaxation (1.75 s), $M_b^0$ is the equilibrium signal intensity, $M_b^{SS}$ is the brain water signal intensity from the labeled image, and $\alpha$ is the labeling efficiency (0.59). $T_{1diff}$ maps were generated based on the comparison of $T_1$WI pre/post contrast:

$$T_{1diff} = \frac{T_{1post} - T_{1pre}}{T_{1pre}} \times 100 \quad (5)$$

where $T_{1pre}$ is the $T_1$-weighted image pre-contrast and $T_{1post}$ is the $T_1$-weighted image post-contrast.

Volumes of interest were drawn using MIPAV (Biomedical Imaging Research Services Section, National Institutes of Health, Bethesda, MD, USA). Individual volumes of interests were drawn for ischemic lesion, the comparable contralateral region, and areas of white matter disease (WMD) on $T_2$, ADC, and CBF parameter maps. The presence of hemorrhage was identified on GRE images. Additional volumes of interests were drawn for regions with enhancement on $T_1$WI after contrast.

## Image Analysis: Histopathology and Immunohistochemistry

For hematoxylin–eosin staining and EB fluorescence, photos were taken using an Axioplan light microscope (Carl Zeiss Microimaging GmbH, Berlin, Germany) at × 5, × 10, × 20, and × 40 magnification in regions positive for lesions, hemorrhage, or BBB disruption on MRI. Additional photos were taken in the equivalent contralateral control region. For double immunofluorescence, photos were taken at × 20 and × 40 for the same locations as for hematoxylin–eosin and EB fluorescence.

For an in-depth characterization of vessel pathology, photos were taken at × 20 magnification in regions positive for lesions on hematoxylin–eosin. Additional photos were taken in 12 locations distributed along the cortex ($n$ = 8) and in the striatum ($n$ = 4). Individual vessels were counted and scored as healthy or abnormal using ImageJ software (NIH, Bethesda, MD, USA). Vessels were considered abnormal if they showed gross morphological changes, hypertrophy, and/or thrombosis. The percentage of hypertrophied and/or thrombosed vessels was calculated for both healthy tissue and lesion.

## Statistics

Values are expressed as mean (s.d.). Normality was tested using the Shapiro–Wilk and Kolmogorov–Smirnov tests.

All lesion analyses were performed using one-way analysis of variance and *post hoc* Tukey tests. Differences in CBF, $T_2$, and ADC were investigated for lesion versus healthy tissue and lesion versus whole brain data. An adjusted *P*-value of 0.025 was considered statistically significant. Additional comparisons were drawn between WMD and whole-brain data. A *P*-value of 0.05 was considered statistically significant. All BBB analyses were performed using Kruskal–Wallis and *post hoc* testing using Mann–Whitney tests. Differences in $T_{1diff}$ were investigated for Gd-enhancing lesions versus healthy tissue and Gd-enhancing CSF. An adjusted *P*-value of 0.017 was considered statistically significant.

## Results

Ten out of 12 (83%) animals were MRI-positive for ischemic lesions. The remaining two were MRI-negative, but had to be euthanized due to cardiac and respiratory distress. The average age of symptom onset was 450 (50) days, or 1.2 (0.1) years (Table 1). Animals had an average of 3 (1) lesions, with a volume of 10 $mm^3$ (10) (range 2–57). Eight out of 10 (80%) animals had additional WMD, with an average volume of 110 $mm^3$ (70) (range 22–215). All lesion-positive animals had hemorrhage present on GRE, the majority unrelated to the site of lesion development. Animals presented with a variety of neurological changes, which typically matched the lesion's location. All animals showed a rough coat or ruffled fur. Animals with striatal lesions had additional lethargy. Animals with visual lesions showed mild incoordination. Animals with thalamic lesions showed no interest in the food. Animals that were lesion-negative also showed a rough coat or ruffled fur, but otherwise appeared healthy with a normal CNS.

Individual lesions were distributed across frontal/prelimbic (3.1%), motorsensory (18.8%), striatal (21.9%), visual (28.1%), auditory (12.5%), and thalamic (12.5%) regions (Figure 2A). The remaining 3.1% of lesions covered multiple categories. The most commonly affected arterial distribution was the middle cerebral artery, occurring in 50% of cases (Figure 2B). The posterior cerebral and anterior cerebral arteries were affected to a lesser extent, occurring in 28% and 6% of cases, respectively. The remaining cases (16%) covered multiple territories.

Lesions appeared hyperintense on $T_2$ (arrows) and ADC (not shown), and hypointense on ASL (dotted outline) (Figure 3). Lesion $T_2$ values (71 ms (6), +25%) and ADC values ($1.1 \times 10^{-3}$ $mm^2/s$ (0.2), +43%) were significantly elevated ($P<0.01$). Accompanying these changes was a significant reduction in CBF (70 mL/100 g/min (30)) when compared with that of healthy tissue (110 mL/100 g/min (40), $P<0.01$) and whole brain (120 mL/100 g/min (30), $P<0.01$). Animals that were lesion-negative had normal CBF (156 mL/100 g/min). Their $T_2$ values (55 ms) and ADC values ($0.77 \times 10^{-3}$ $mm^2/s$) were also normal.

Bilateral WMD was present in 75% of WMD-positive animals. The remaining 25% had WMD confined to a single hemisphere. Similar to findings for individual lesions, WMD appeared hyperintense on $T_2$ and ADC, and hypointense on ASL. WMD $T_2$ values (82 ms (5)) and ADC values ($1.4 \times 10^{-3}$ $mm^2/s$ (0.1)) were significantly elevated when compared with that of healthy tissue ($P<0.01$). CBF values were significantly reduced (50 mL/100 g/minute (30)) when compared with that of healthy tissue ($P<0.01$).

A large proportion of lesions (62.5%) were coincident with BBB disruption—these regions appeared hyperintense (arrows) on $T_{1diff}$ (Figure 3, bottom row). The average signal intensity increase was 20% (9) (range 7–36), significantly higher than the 5% (4) in healthy tissue ($P<0.01$). In a subset of animals, additional enhancement was observed in the CSF

**Table 1** SHRSP animal characteristics and cerebrovascular events

| *Animal number* | *DOB* | *Neurological status* | | *Imaging* | *No. of lesions* | *WMD* |
|---|---|---|---|---|---|---|
| | | *DOE* | *Details*[a] | | | |
| 1–24 | 09/27/2005 | 10/30/2006 | 1, 3, 4 | 11/02/2006 | 5 | Y |
| 2–25 | 10/20/2005 | 11/02/2006 | 1, 2 | 11/02/2006 | 1 | N |
| 3–26 | 09/24/2005 | 11/07/2006 | 1, 4, 6 | 11/09/2006 | 4 | Y |
| 4–27 | 09/24/2005 | 11/07/2006 | 1, 4, 6 | 11/09/2006 | 4 | Y |
| 5–29 | 09/30/2005 | 11/30/2006 | 1, 3 facial muscle fasciculations no interest in food | 12/01/2006 | 4 | Y |
| 6–32 | 09/23/2005 | 01/15/2007 | 1 | 01/18/2007 | 3 | Y |
| 7–33 | 10/11/2005 | 01/17/2007 | 1, 2 | 01/18/2007 | 5 | Y |
| 8–34 | 09/23/2005 | 01/20/2007 | 1, 2 | 01/20/2007 | 2 | Y |
| 9–37 | 09/23/2005 | 02/20/2007 | 1 | 02/23/2007 | 2 | Y |
| 10–38 | 09/23/2005 | 02/20/2007 | 1, 5, 6 | 02/23/2007 | 2 | N |
| 11–35 | 09/23/2005 | NA | 1 cardiac/respiratory distress | 03/08/2007 | 0 | N |
| 12–36 | 09/23/2005 | NA | 1 cardiac/respiratory distress | 03/08/2007 | 0 | N |

DOE, date of event; NA, not applicable; SHRSP, spontaneously-hypertensive, stroke-prone; WMD, white matter disease.
[a]1 = rough coat; 2 = lethargy; 3 = hunched posture; 4 = mild incoordination; 5 = falling to one side; 6 = porphyrin+.

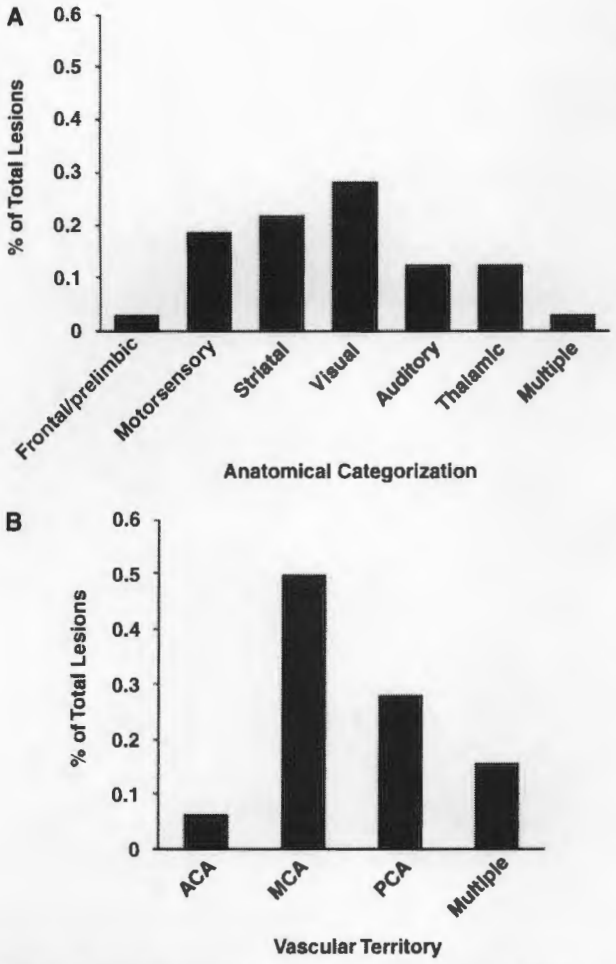


**Figure 2** Categorical and vascular distribution of lesions in SHRSP rats. Individual lesions were distributed across frontal/prelimbic (3.1%), motorsensory (18.8%), striatal (21.9%), visual (28.1%), auditory (12.5%), and thalamic (12.5%) regions. The remaining 3.1% of lesions covered multiple categories. The most commonly affected arterial distribution was the middle cerebral artery, occurring in 50% of cases. ACA, anterior cerebral artery; MCA, middle cerebral artery; PCA, posterior cerebral artery.

space, more prominent in the lateral ventricles than that of the third and fourth ventricles. The average signal intensity increase was 20% (10) (range 11–36), comparable to that of Gd-enhancing lesions ($P=0.268$).

For lesioned areas we observed the presence of thrombi and/or compressed vessels (Figure 4). Lesions on hematoxylin–eosin had a spongy appearance, with tissue rarefaction and vacuolization, indicating the presence of vasogenic edema. More than half of the vessels (56.1%) appeared hyperplastic, some with additional thrombosis (Figure 4, top row, asterisks) and diapedesis of blood. Affected vessels were 100 to 250 $\mu$m in diameter (average 150 $\mu$m (40)). This is in comparison to the 3.1% of hyperplastic vessels in healthy tissue of the same animal. EB extravasation was limited to the immediate area surrounding the thrombosed vessel. The remainder of the lesion was EB-negative with an intact BBB. Other vessels were significantly compressed (Figure 4, bottom row, arrows). EB extravasation was present, evident by neuronal uptake throughout portions of the lesion. This lesion was EB-positive with a disrupted BBB.

In areas with disrupted BBB, loss of Reca-1/laminin staining was observed when compared with healthy contralateral regions (Figure 5). For healthy parenchyma (Figure 5, top row), the endothelium and extracellular matrix were continuous, with a normal morphological appearance. Both Reca-1 and laminin staining were intense. For the striatal lesion that had no evidence of BBB disruption on $T_{1diff}$, there was a complete loss of laminin staining. However, Reca-1 staining remained intact and was at the same intensity as that in healthy parenchyma. For the thalamic lesion that had evidence of BBB breakdown on $T_{1diff}$, there was loss of both Reca-1 and laminin staining.

## Discussion

Hypertension is the leading modifiable risk factor for ischemic stroke, both clinically (Bogousslavsky *et al*, 1988; Sacco *et al*, 1997) and experimentally (Barone *et al*, 1992). In SHRSP rats, hypertension begins to develop around 1 to 2 months of age and becomes malignant (arterial BP >200 mm Hg) by 4 to 6 months (Yamori *et al*, 1976*a*). There are dramatic changes in the vascular tree, with dysfunction likely occurring prior to development of overt neurological symptoms or evidence of disease on MRI. This dysfunction begins on a biochemical level, with intrinsic abnormalities in $Na^+$ handling and ion transport in the kidney (Graf *et al*, 1993). Secondary to changes in the kidney are changes in the mechanics and functionality of the arterial vessels supplying the brain, particularly in terms of myogenic tone and vascular compliance (Ibrahim *et al*, 2006; Legrand *et al*, 1993). SHRSP have less collateralization and the medial/lumen ratio is significantly decreased in comparison to their normotensive counterparts (Coyle, 1987; Coyle and Heistad, 1991). With age the vessels ultimately become less responsive to stress and more vulnerable to permanent irreversible damage. Dysfunction of the vascular tree is exacerbated, increasing the risk of chronic hypoperfusion and subsequent stroke.

In this study, we observed a consistent and significant decrease in CBF after spontaneous stroke in aged SHRSP rats on a standard diet (no supplemental salt). All lesions had reduced CBF in comparison to healthy tissue and were characterized by hyperplastic, thrombosed, and compressed vessels/microvessels. These findings suggest ischemic lesion development and support the theory of slow disease progression as the mechanism of injury. Although we cannot rule out the possibility of lesion development occurring as a result of an acute event such as a spike

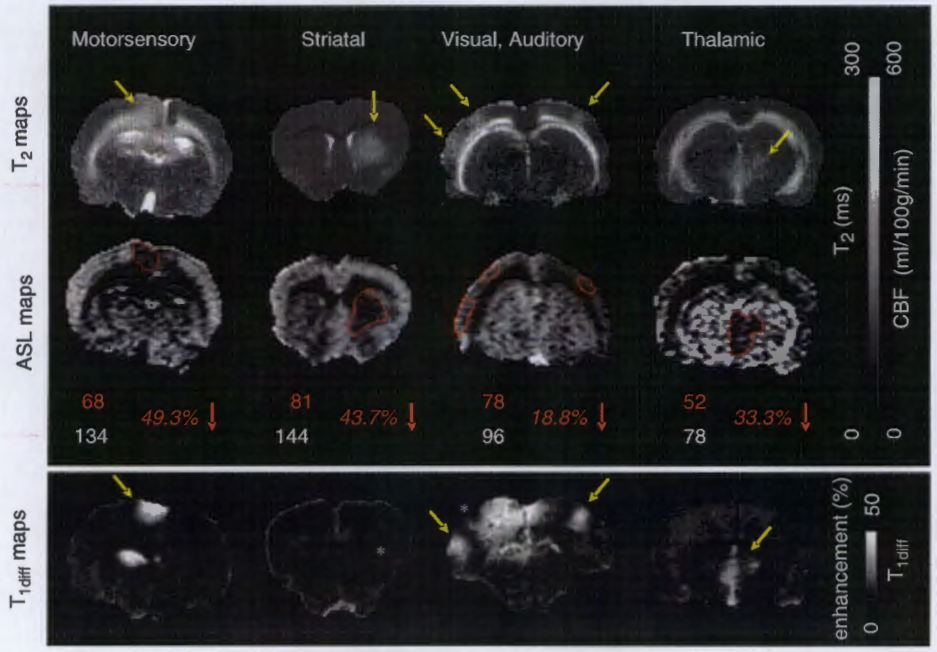


**Figure 3** MRI lesion distribution and characteristics in SHRSP rats. Lesions appeared hyperintense (arrows) on $T_2$ and hypointense on ASL (red outline) in contrast to healthy tissue. Lesions had significantly reduced CBF values when compared with those in healthy tissue. Lesions coincident with BBB disruption appeared hyperintense (arrows) on $T_{1diff}$. Lesions with an intact BBB showed no evidence of enhancement (asterisks).

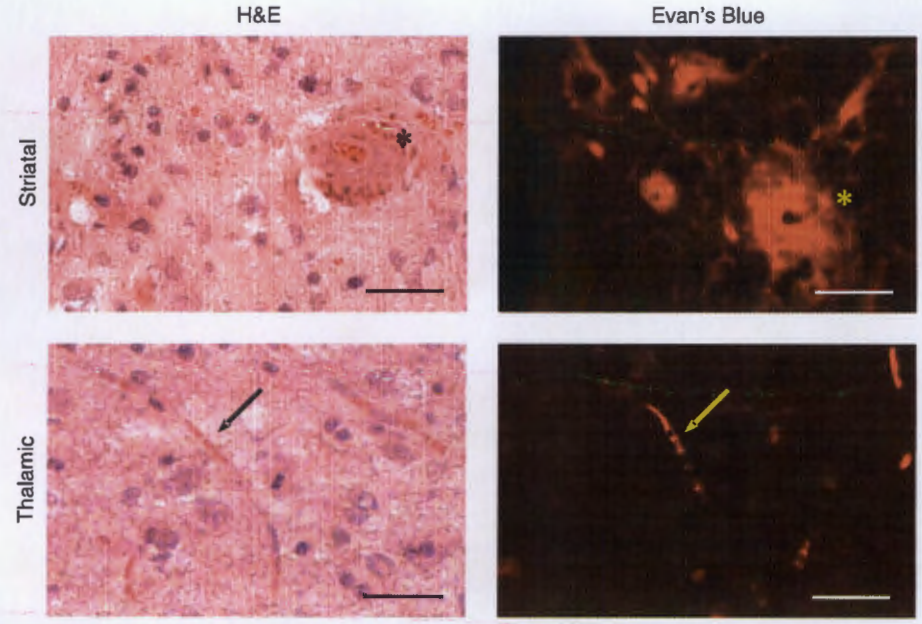


**Figure 4** Histopathological evaluation of vascular remodeling. Hematoxylin–eosin (left) and EB (right) provide evidence of hypertension-induced vascular remodeling present in aged SHRSP rats with spontaneous stroke. In MRI-confirmed stroke regions, vessels were clotted (asterisks), compressed (arrows), and hypertrophied (asterisks). Regions with BBB disruption on MRI were well-correlated with the extravasation of EB. Scale bar = 100 $\mu$m (top images, × 20) and 50 $\mu$m (bottom images, × 40).

in BP, or perhaps a combination of both ischemia and loss of CBF autoregulation, our results are comparable to previous reports in SHRSP using autoradiography (Katayama *et al*, 1997; Mies *et al*, 1999) or the hydrogen clearance method (Yamori and Horie, 1977). In lesion areas we observed an approximate 40% reduction in flow. This may indicate that some lesions have had spontaneous but incomplete

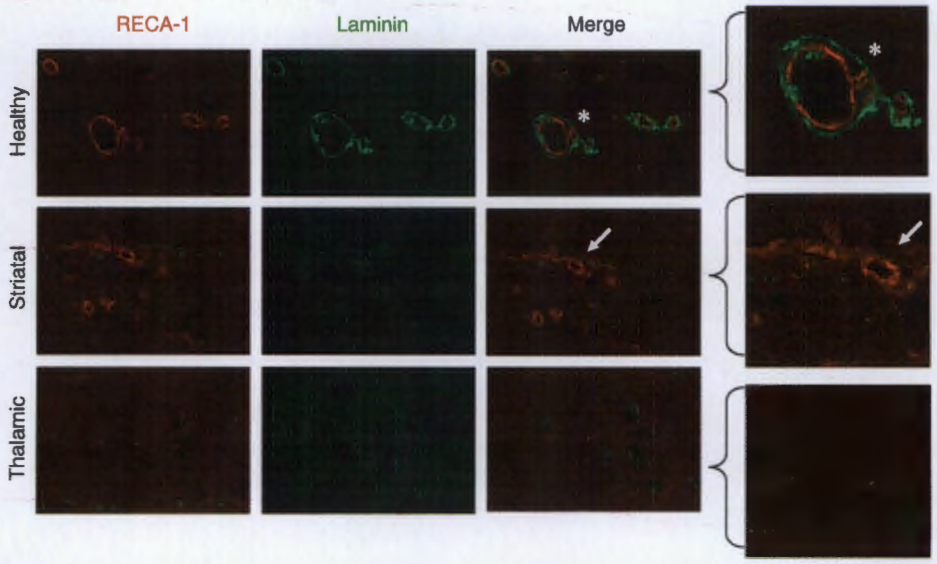


**Figure 5** Immunofluorescence of BBB disruption. Laminin and Reca-1 double immunofluorescence was performed for assessment of the extracellular matrix (laminin, green) and endothelium (Reca-1, red). Healthy tissue had intact ECM and endothelium in the parenchyma. These areas were $T_{1diff}$-negative. The affected regions showed loss of laminin staining and/or loss of Reca-1 staining. Images = × 40. Those with loss of both laminin and Reca-1 staining were $T_{1diff}$-positive.

reperfusion. It may also indicate that this flow reduction is not at the level related to cytotoxic edema, which would be observable as an ADC decline (Moseley *et al*, 1990). However, a persistence of a mild-to-moderate flow reduction would result in permanent damage in a delayed manner (Hossmann, 1994). Interestingly, a few animals had reduced perfusion not only in the lesion but also across the entire brain. In healthy tissue, our flow measurements were comparable to that in both SHR (Danker and Duong, 2007; Wei *et al*, 1992) and disease-negative SHRSP (Mies *et al*, 1999). No increase in CBF was observed in our study.

Our findings are in dramatic contrast to prior work employing young SHRSP rats on a high-salt diet (Blezer *et al*, 1998*a*; Guerrini *et al*, 2002; Smeda *et al*, 1999). In these studies, SHRSP rats develop lesions 4 to 6 weeks after the start of salt-loading. During this 4- to 6-week time frame, their BP increases dramatically from around 160–180 mm Hg to greater than 220 mm Hg, beyond the limit of CBF autoregulation. Observations have been made suggesting that lesion development is edematous in nature, on the basis of an increase in CBF prior to lesion development and persisting long afterwards (Smeda *et al*, 1999). One possible explanation for the difference is salt loading and its effect on the kidney. As the kidney is the major system maintaining ion homeostasis and BP, overloading the SHRSP system with $Na^+$ induces a dramatic loss in osmotic balance, a significant increase in BP, and subsequent hyperperfusion (Mori *et al*, 2008). Massive influx of water leads to swelling and global rather than focal edema, with tissue damage secondary to BBB disruption.

Additional support for the ischemic pathway is our observance of individual lesions in focal anatomical areas limited to specific vascular territories, namely the middle cerebral artery, posterior cerebral artery, and anterior cerebral artery. Similar to the clinical setting, the highest frequency of lesions occurred in the middle cerebral artery territory (Bogousslavsky *et al*, 1988). Lesions predominantly occurred in the motorsensory, striatal, and visual regions, and to a lesser extent in the thalamic and auditory regions. On the basis of the diameter of affected vessels, lesion size and distribution, and neurological symptoms, it is likely that stroke progression in SHRSP is a combination of small-artery and large-artery disease. Again, these findings are in contrast to SHRSP rats on a high-salt diet. SHRSP rats on a high-salt diet found positive for disease have a preponderance of lesions located in the striatum, with extensive WMD and brain swelling (Guerrini *et al*, 2002; Sironi *et al*, 2004). In many cases the appearance of the lesions on MRI is somewhat diffuse and non-specific. Histologically these lesions had significant neuronal loss, astrocytic prominence, and extensive deposition of fibrinoid–eosinophilic material in the neuropil. In our study, spontaneous lesions had the same histological characteristics as lesions from mechanical induction of stroke (Guerrini *et al*, 2002). Deposition of fibrinoid–eosinophilic material was not observed.

Another interesting finding in our study was the greater extent of BBB disruption observed in comparison with previous work using SHRSP rats (Lee *et al*, 2007; Sironi *et al*, 2004). BBB disruption evident on $T_{1diff}$ was coincident with 62.5% of lesions and generally affected the entire lesion volume. The

affected areas had disruption of both extracellular matrix and endothelium, most likely related to matrix metalloproteinase upregulation after stroke (Fukuda *et al*, 2004; Rosenberg *et al*, 1998). Those areas that were BBB-negative according to $T_{1diff}$ did show disruption of the extracellular matrix, but a relatively normal-appearing endothelium. In these cases, it is likely that the BBB is leaky, but perhaps not leaky to Gd contrast. Gd–DTPA has a molecular weight of 590 Da and does not readily cross the intact BBB. It is possible and very likely that the BBB would be leaky to molecules and proteins of lower molecular weight, so we cannot conclude that the BBB is intact when the post-contrast $T_1$ appears negative.

It is important to note that we imaged at a single time point after development of neurological symptoms. Given the difficulty in 'catching' the occurrence of lesions in the acute rather than subacute-to-chronic phase of stroke, it is not surprising that we were unable to observe the ADC decline associated with cytotoxic edema. Another possibility for not observing the ADC decline and observing rather a normal or increased ADC, is spontaneous reperfusion. In patients, spontaneous recanalization and reperfusion occurs in up to 50% of cases within 24 h of stroke onset (Kassem-Moussa and Graffagnino, 2002; Merino *et al*, 2008). We imaged within 1 to 3 days of symptom onset based on the availability of MRI, so partial reperfusion of the affected territory is a feasible explanation. Although difficult and time consuming, longitudinal imaging studies of SHRSP rats, before and throughout disease progression, should help refine our understanding of the natural history of stroke in this model. Simultaneous BP measurements will be integral in determining the association (if any) between BP changes and lesion development.

Our observations and conclusions are limited to stroke progression in aged, female SHRSP rats. Unfortunately aged male SHRSP rats were not available at the inception of our study due to a gap in breeding cycles. We have recently observed a similar incidence and distribution of lesion development in aged male SHRSP rats, although at a much younger age (~9 months) than the female rats presented here (over 1 year). This is supported by recent work using SHRSP rats confirming gender-related differences in myogenic tone and endothelial dysfunction, and increased susceptibility to stroke in males versus females (Ibrahim *et al*, 2006; Masineni *et al*, 2005).

We should also note that although the pattern of lesion development in SHRSP rats in our study is similar to that in acute stroke patients reporting at the clinic, we observed stroke in 10 out of 12 (83%) animals. This is dramatically higher than the prevalence of stroke in humans. One major difference is that the SHRSP rat is a genetic model of hypertension, with 100% incidence of high BP in young adults. In contrast, humans have a 31.3% incidence of natural hypertension (age-adjusted). More than half of humans develop high BP at ages 45 and over, not as young adults. Another difference is that the majority of SHRSP rats develop associated heart, lung, and kidney disease; and those animals that do not develop stroke die of complications related to end-organ damage. While cardiovascular and renal diseases are common in acute stroke patients reporting at the clinic, they occur at a much higher rate in SHRSP rats. Additional study of other affected organ systems, such as heart, kidney, and lungs, in SHRSP animals should help to understand the nuances in the mechanism(s) of hypertensive pathology and the link to stroke development.

In summary, the findings of our study suggest that lesion development in SHRSP rats is ischemic in nature and is related to both hypertension-induced vascular remodeling and persistent hypoperfusion. This model should be useful for studying the relationship between chronic hypertension and BBB dysfunction in stroke, both in terms of primary and secondary prevention. A high proportion of acute stroke patients coming into the emergency room have been taking a variety of medications for hypertension (e.g., ACE inhibitors), high cholesterol (e.g., statins) heart disease (e.g., blood thinners), and so on. Future study should, therefore, include analyzing the effects of therapeutic intervention at the onset of hypertension versus late-stage disease. This will allow us to determine whether the disease process can be reversed with delayed intervention and thereby reduce the prevalence of stroke.

## Acknowledgements

This research was supported by the Division of Intramural Research of the National Institute of Neurological Disorders and Stroke, National Institutes of Health. We thank Afonso C Silva, PhD, and Fernando P Paiva, PhD, for assistance in ASL optimization and setup. We also thank Christl A Ruetzler, BA, for advice on histological analysis and Ashleigh R Martin, BA, for assistance in MRI analysis.

## Disclosure/conflict of interest

The authors declare no conflict of interest.

## References

Barone FC, Price WJ, White RF, Willette RN, Feuerstein GZ (1992) Genetic hypertension and increased susceptibility to cerebral ischemia. *Neurosci Biobehav Rev* 16:219–33

Biezer EL, Nicolay K, Bar D, Goldschmeding R, Jansen GH, Koomans HA, Joles JA (1998*a*) Enalapril prevents imminent and reduces manifest cerebral edema in stroke-prone hypertensive rats. *Stroke* 29:1671–7; discussion 1677–1678

Blezer EL, Schurink M, Nicolay K, Bar PR, Jansen GH, Koomans HA, Joles JA (1998*b*) Proteinuria precedes cerebral edema in stroke-prone rats: a magnetic resonance imaging study. *Stroke* 29:167–74

Bogousslavsky J, Van Melle G, Regli F (1988) The Lausanne Stroke Registry: analysis of 1,000 consecutive patients with first stroke. *Stroke* 19:1083–92

Coyle P (1987) Dorsal cerebral collaterals of stroke-prone spontaneously hypertensive rats (SHRSP) and Wistar Kyoto rats (WKY). *Anat Rec* 218:40–4

Coyle P, Heistad DD (1991) Development of collaterals in the cerebral circulation. *Blood Vessels* 28:183–9

Danker JF, Duong TQ (2007) Quantitative regional cerebral blood flow MRI of animal model of attention-deficit/hyperactivity disorder. *Brain Res* 1150:217–24

Fredriksson K, Auer RN, Kalimo H, Nordborg C, Olsson Y, Johansson BB (1985) Cerebrovascular lesions in stroke-prone spontaneously hypertensive rats. *Acta Neuropathol* 68:284–94

Fukuda S, Fini CA, Mabuchi T, Koziol JA, Eggleston LL, Jr, del Zoppo GJ (2004) Focal cerebral ischemia induces active proteases that degrade microvascular matrix. *Stroke* 35:998–1004

Graf C, Maser-Gluth C, de Muinck Keizer W, Rettig R (1993) Sodium retention and hypertension after kidney transplantation in rats. *Hypertension* 21:724–30

Guerrini U, Sironi L, Tremoli E, Cimino M, Pollo B, Calvio AM, Paoletti R, Asdente M (2002) New insights into brain damage in stroke-prone rats: a nuclear magnetic imaging study. *Stroke* 33:825–30

Hilbert P, Lindpaintner K, Beckmann JS, Serikawa T, Soubrier F, Dubay C, Cartwright P, De Gouyon B, Julier C, Takahasi S, Vincent M, Ganten D, Georges M, Lathrop GM (1991) Chromosomal mapping of two genetic loci associated with blood-pressure regulation in hereditary hypertensive rats. *Nature* 353:521–9

Hossmann KA (1994) Viability thresholds and the penumbra of focal ischemia. *Ann Neurol* 36:557–65

Ibrahim J, McGee A, Graham D, McGrath JC, Dominiczak AF (2006) Sex-specific differences in cerebral arterial myogenic tone in hypertensive and normotensive rats. *Am J Physiol Heart Circ Physiol* 290:H1081–9

Jesmin S, Maeda S, Mowa CN, Zaedi S, Togashi H, Prodhan SH, Yamaguchi T, Yoshioka M, Sakuma I, Miyauchi T, Kato N (2007) Antagonism of endothelin action normalizes altered levels of VEGF and its signaling in the brain of stroke-prone spontaneously hypertensive rat. *Eur J Pharmacol* 574:158–71

Kassem-Moussa H, Graffagnino C (2002) Nonocclusion and spontaneous recanalization rates in acute ischemic stroke: a review of cerebral angiography studies. *Arch Neurol* 59:1870–3

Katayama Y, Katsumata T, Muramatsu H, Usuda K, Obo R, Terashi A (1997) Effect of long-term administration of ethyl eicosapentate (EPA-E) on local cerebral blood flow and glucose utilization in stroke-prone spontaneously hypertensive rats (SHRSP). *Brain Res* 761:300–5

Kim S, Tokuyama M, Hosoi M, Yamamoto K (1992) Adrenal and circulating renin–angiotensin system in stroke-prone hypertensive rats. *Hypertension* 20:280–91

Lee JM, Zhai G, Liu Q, Gonzales ER, Yin K, Yan P, Hsu CY, Vo KD, Lin W (2007) Vascular permeability precedes spontaneous intracerebral hemorrhage in stroke-prone spontaneously hypertensive rats. *Stroke* 38:3289–91

Legrand MC, Benessiano J, Levy BI (1993) Endothelium, mechanical compliance, and cGMP content in the carotid artery from spontaneously hypertensive rats. *J Cardiovasc Pharmacol* 21(Suppl 1):S26–30

Masineni SN, Chander PN, Singh GD, Powers CA, Stier CT, Jr (2005) Male gender and not the severity of hypertension is associated with end-organ damage in aged stroke-prone spontaneously hypertensive rats. *Am J Hypertens* 18:878–84

Merino JG, Latour LL, An L, Hsia AW, Kang DW, Warach S (2008) Reperfusion half-life: a novel pharmacodynamic measure of thrombolytic activity. *Stroke* 39:2148–50

Mies G, Hermann D, Ganten U, Hossmann KA (1999) Hemodynamics and metabolism in stroke-prone spontaneously hypertensive rats before manifestation of brain infarcts. *J Cereb Blood Flow Metab* 19:1238–46

Mori T, Polichnowski A, Glocka P, Kaldunski M, Ohsaki Y, Liang M, Cowley AW, Jr (2008) High perfusion pressure accelerates renal injury in salt-sensitive hypertension. *J Am Soc Nephrol* 19:1472–82

Moseley ME, Cohen Y, Mintorovitch J, Chileuitt L, Shimizu H, Kucharczyk J, Wendland MF, Weinstein PR (1990) Early detection of regional cerebral ischemia in cats: comparison of diffusion- and T2-weighted MRI and spectroscopy. *Magn Reson Med* 14:330–46

Okamoto K, Yamori Y, Nagaoka A (1974) Establishment of the stroke-prone spontaneously hypertensive rats (SHR). *Circ Res* 34:143–53

Orlov SN, Adarichev VA, Devlin AM, Maximova NV, Sun YL, Tremblay J, Dominiczak AF, Postnov YV, Hamet P (2000) Increased Na(+)/H(+) exchanger isoform 1 activity in spontaneously hypertensive rats: lack of mutations within the coding region of NHE1. *Biochim Biophys Acta* 1500:169–80

Rosenberg GA, Estrada EY, Dencoff JE (1998) Matrix metalloproteinases and TIMPs are associated with blood-brain barrier opening after reperfusion in rat brain. *Stroke* 29:2189–95

Sacco RL, Roberts JK, Boden-Albala B, Gu Q, Lin IF, Kargman DE, Berglund L, Hauser WA, Shea S, Paik MC (1997) Race–ethnicity and determinants of carotid atherosclerosis in a multiethnic population. The Northern Manhattan Stroke Study. *Stroke* 28:929–35

Savage P, Jeng AY (2002) Upregulation of endothelin-1 binding in tissues of salt-loaded stroke-prone spontaneously hypertensive rats. *Can J Physiol Pharmacol* 80:470–4

Silva AC, Kim SG (1999) Pseudo-continuous arterial spin labeling technique for measuring CBF dynamics with high temporal resolution. *Magn Reson Med* 42:425–9

Sironi L, Guerrini U, Tremoli E, Miller I, Gelosa P, Lascialfari A, Zucca I, Eberini I, Gemeiner M, Paoletti R, Gianazza E (2004) Analysis of pathological events at the onset of brain damage in stroke-prone rats: a proteomics and magnetic resonance imaging approach. *J Neurosci Res* 78:115–22

Sironi L, Tremoli E, Miller I, Guerrini U, Calvio AM, Eberini I, Gemeiner M, Asdente M, Paoletti R, Gianazza E (2001) Acute-phase proteins before cerebral ischemia in stroke-prone rats: identification by proteomics. *Stroke* 32:753–60

Smeda JS, VanVliet BN, King SR (1999) Stroke-prone spontaneously hypertensive rats lose their ability to auto-regulate cerebral blood flow prior to stroke. *J Hypertens* 17:1697–705

Sonalker PA, Tofovic SP, Jackson EK (2004) Increased expression of the sodium transporter BSC-1 in

spontaneously hypertensive rats. *J Pharmacol Exp Ther* 311:1052–61

Tamaki K, Sadoshima S, Baumbach GL, Iadecola C, Reis DJ, Heistad DD (1984) Evidence that disruption of the blood–brain barrier precedes reduction in cerebral blood flow in hypertensive encephalopathy. *Hypertension* 6:I75–81

Wei L, Lin SZ, Tajima A, Nakata H, Acuff V, Patlak C, Pettigrew K, Fenstermacher J (1992) Cerebral glucose utilization and blood flow in adult spontaneously hypertensive rats. *Hypertension* 20:501–10

Yamori Y, Horie R (1977) Developmental course of hypertension and regional cerebral blood flow in stroke-prone spontaneously hypertensive rats. *Stroke* 8:456–61

Yamori Y, Horie R, Handa H, Sato M, Fukase M (1976*a*) Pathogenetic similarity of strokes in stroke-prone spontaneously hypertensive rats and humans. *Stroke* 7: 46–53

Yamori Y, Horie R, Sato M, Handa H (1976*b*) Proceedings: regional cerebral blood flow in stroke-prone SHR: a preliminary report. *Jpn Heart J* 17:378–80